nature neuroscience

Oxidation of a potassium channel causes progressive sensory function loss during aging

Shi-Qing Cai & Federico Sesti

Potassium channels are key regulators of neuronal excitability. Here we show that oxidation of the K^+ channel KVS-1 during aging causes sensory function loss in *Caenorhabditis elegans* and that protection of this channel from oxidation preserves neuronal function. Chemotaxis, a function controlled by KVS-1, was significantly impaired in worms exposed to oxidizing agents, but only moderately affected in worms harboring an oxidation-resistant KVS-1 mutant (C113S). In aging C113S transgenic worms, the effects of free radical accumulation were significantly attenuated compared to those in wild type. Electrophysiological analyses showed that both reactive oxygen species (ROS) accumulation during aging and acute exposure to oxidizing agents acted primarily to alter the excitability of the neurons that mediate chemotaxis. Together, these findings establish a pivotal role for ROS-mediated oxidation of voltage-gated K^+ channels in sensorial decline during aging in invertebrates.

Oxidative metabolism leads to the production of highly reactive oxygen species (ROS), which are important in the physiology and pathophysiology of the nervous system. With the passage of time, the redox environment of neurons can be altered in favor of oxidation by an increased production of ROS or by a decreased activity of antioxidant defenses, which include both enzymatic and nonenzymatic antioxidants. This condition, which is known as oxidative stress, is thought to represent a general contributing factor to aging in biological systems[1]. Uncontrolled ROS can cause considerable damage to proteins, DNA and cell membranes[1]. Oxidative damage may not only contribute to the mechanisms leading to the progressive sensory and cognitive function loss that is part of the normal aging process, but has also been implicated in neurodegeneration characteristic of diseases such as Alzheimer's[2].

K^+ channels are essential to neuronal function and survival. It is possible that the interaction of ROS with K^+ channels may cause modifications of membrane currents and potentials, thereby leading to neuronal dysfunction. Many K^+ channels, including voltage-gated channels[3], 2-P domains channels[4], BK channels[5] and GIRK channels[6], can be modified by oxidizing agents *in vivo* and *in vitro*. However, with the exception of a few studies that suggest a potential role for oxidation of K^+ channels during neuronal hypoxia[7,8], the notion that modification of K^+ channels by ROS can be a mechanism of neurodegeneration has remained an intriguing but unproven hypothesis.

To address the fundamental question of whether K^+ channels can be physiological targets of ROS and whether these interactions may have a role in the mechanisms underlying age-related neurodegeneration, we used the metazoan *C. elegans* because it is a well established model for studying biological processes related to aging[9]. In particular, the nervous system of the worm expresses KVS-1, a voltage-gated K^+ channel whose physiological characteristics—it is crucial for the maintenance and sensitivity of the nervous system of the worm[10]—make it a prime candidate for investigating the impact of oxidation of voltage-gated K^+ channels on neuronal function.

We show that modification of KVS-1 by endogenous ROS during aging leads to sensorial decline and that protection of this channel from oxidation preserves neuronal function.

RESULTS

KVS-1 is susceptible to redox modulation

Whole-cell KVS-1 currents, elicited in Chinese hamster ovary cells by voltage steps from–80 mV (holding voltage) to +120 mV in 20-mV increments, exhibited rapid acitvation and inactivation kinetics (**Fig. 1a**). Exposure for 5 min to the oxidizing agent chloramine-T (CHT) in the bath solution slowed inactivation of KVS-1 (time constant $\tau = 33 \pm 5.2$ ms and $\tau = 91 \pm 15$ ms at +120 mV in control and CHT, respectively; $n = 3$; **Fig. 1a**). CHT modifications could not be reversed by washout with CHT-free bath solution (data not shown), but subsequent application of dithiothreitol (DTT) reversed them within 5–10 min (**Fig. 1a**; $\tau = 35 \pm 6.1$, n = 3). Unlike other A-type channels, KVS-1 possesses a domain in front of the N-terminal inactivation domain, the N-type regulatory domain (NIRD), which acts to slow N-type inactivation[11,12]. Therefore, we performed quantitative analysis using a NIRD-deleted mutant (ΔNIRD), which inactivates faster than the wild type[11]. CHT (**Supplementary Table 1** online) or the more physiologically relevant hydrogen peroxide (**Fig. 1b**) slowed inactivation tenfold, whereas DTT restored original kinetics. H_2O_2 and CHT led to a moderate (20%) increase in the peak current and did not shift the half-maximal voltage for activation, $V_{1/2}$ (**Supplementary Table 1**).

Department of Physiology and Biophysics, Robert Wood Johnson Medical School, University of Medicine and Dentistry of New Jersey, Piscataway, New Jersey, USA. Correspondence should be addressed to F.S. (sestife@umdnj.edu).

Received 5 January; accepted 9 February; published online 29 March 2009; doi:10.1038/nn.2291

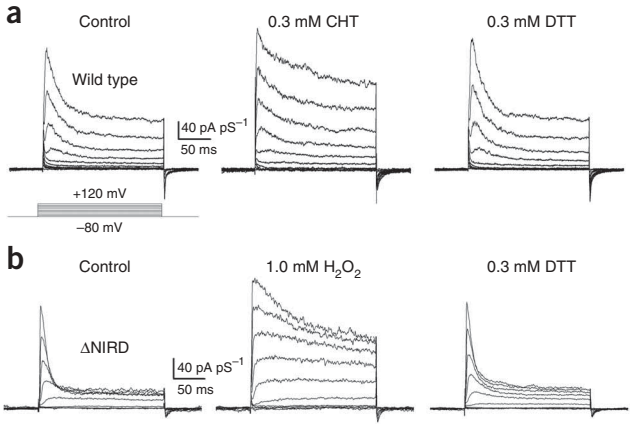

Figure 1 KVS-1 channels expressed in mammalian cells are susceptible to redox modulation. (**a**) Representative macroscopic KVS-1 currents elicited by voltage jumps from –80 mV to +120 mV in 20 mV increments (inset) in control and after application of 0.3 mM CHT for 5 min in the test solution, washout and application of 0.3 mM DTT for 5–10 min in the test solution. (**b**) Representative ΔNIRD currents in control and after application of 1 mM H_2O_2 for 2–3 min, washout, and application of 0.3 mM DTT for 5–10 min.

To determine which residues were modified by H_2O_2 and CHT, we focused on the six endogenous cysteines of KVS-1 as the most likely candidates. Mutation to serine of a conserved cysteine at position 113 in full-length KVS-1 or position 95 in ΔNIRD (C113S or ΔNIRD-C95S) yielded channels that were markedly resistant to H_2O_2 and CHT without affecting other channel attributes (C113S, **Fig. 2a**; $\tau = 30 \pm 4.2$ ms, $\tau = 38 \pm 5.4$ ms and $\tau = 33 \pm 5.0$ at +120 mV in control, CHT and DTT, respectively; $n = 3$, ΔNIRD-C95S, **Fig. 2b** and **Supplementary Table 1**). Mutation of three other cysteines in the full-length channel (C151S and C209S, located in the N-terminal domain; C283S in the middle of the S2 transmembrane domain) did not affect the oxidant susceptibility of the channel. The C172S C173S double mutant showed negligible currents (data not shown), and we did not investigate it further. ΔNIRD-C95S channels showed a significant residual response to oxidation ($P < 0.039$; **Supplementary Table 1**), which may arise from oxidation of non-cysteine residues; we did not investigate this residual response further here.

In the nervous system of *C. elegans*, KVS-1 forms heteromeric complexes with the accessory subunit MPS-1, which acts to modulate functional attributes of the complex, including inactivation[10]. Complexes formed with MPS-1 and wild-type KVS-1 (data not shown) or ΔNIRD (**Supplementary Table 1**) retained susceptibility to CHT, and MPS-1 did not confer redox susceptibility on C113S channels (data not shown) or ΔNIRD-C95S channels (**Supplementary Table 1**). Taken together, these data indicated that mutation of a single cysteine, Cys113, made KVS-1 channels substantially resistant to oxidation and that the accessory subunit MPS-1 did not contribute to this modulation.

The C113S mutant protects chemotaxis

To probe the physiological role of the redox sensitivity of KVS-1 in the nervous system, we constructed transgenic worms expressing wild-type or C113S KVS-1 under the *kvs-1* promoter (P_{kvs-1}) in a *kvs-1* knockout (*tm2034* allele) background. We named these transgenic worms, respectively, *wild type-KVS-1* and *C113S-KVS-1*, and assessed how oxidation challenges affected their physiology. To this end we focused on chemotaxis to water-soluble attractants, a sensory function that is dependent on KVS-1 (ref. 10). Chemotaxis is particularly amenable to study the effects that modifications in the function of KVS-1 have on behavior because the electrical properties of the cells that mediate the primary chemotactic response (and that express KVS-1), the ASE neurons[13], have been extensively characterized *in vivo*[14]. Furthermore several genetic tools, including promoters that express exclusively in the ASE neurons[15,16], GFP reporters[15] and loss-of-function strains, such as the *eat-4(ky5)*, which harbors a mutation in a vesicular glutamate transporter necessary for glutamatergic neurotransmission in *C. elegans*[17], are also available. Consistent with previous results obtained with RNA interference[10], *kvs-1* null worms showed defective chemotaxis to biotin (**Fig. 3a**) and lysine (data not shown). These phenotypes were suppressed in either *wild type-KVS-1* or *C113S-KVS-1* genotypes (**Fig. 3a**), confirming our transgenic approach.

Next, we investigated the effects of H_2O_2 or CHT on chemotaxis. Both oxidants (**Fig. 3b,c**) induced a significant loss of function in all genotypes (on average, 70%) except *C113S-KVS-1*, in which loss was less marked (35%). These effects were not due to the attractant used because switching to lysine yielded similar results (70% versus 31%, only H_2O_2, $n = 3$ experiments; data not shown). Hydrogen peroxide also slightly affected chemotaxis to biotin in *kvs-1* knockout worms (**Fig. 3b**). This indicates that there were cellular components independent of KVS-1 that contributed marginally to the oxidation-mediated decline in chemotaxis.

KVS-1 is expressed in ventral cord motor neurons that contribute to the worm's spontaneous locomotion[10]. This raised the possibility that ROS-mediated impairment of locomotor function might have affected chemotaxis. To exclude or quantify possible effects due to defective locomotion, we expressed wild-type and C113S KVS-1 primarily in the ASE neurons by the means of the *flp-6* promoter, P_{flp-6} (ref. 16) (we named these transgenic worms P_{flp-6}*::wild type-KVS-1* and P_{flp-6}*::C113S-KVS-1*) and assessed their ability to perform chemotaxis to biotin, in ordinary conditions and after exposure to H_2O_2. The chemotactic response of the P_{flp-6}*::wild type-KVS-1* and P_{flp-6}*::C113S-KVS-1* worms recapitulated the response of the *wild type-KVS-1* and *C113S-KVS-1* genotypes (compare **Fig. 3d** with **Fig. 3b**), thereby excluding possible effects on chemotaxis due to defective motor neuron function and locomotion. To independently test the notion that chemotaxis was not affected by defects in locomotion we characterized the latter by counting thrashes[18] and by calculating the worm's average speed on solid substrate[19] (even though chemotaxis is also dependent upon the number of pirouettes and runs[20], these traits receive a substantial contribution from the ASE neurons[21] and therefore

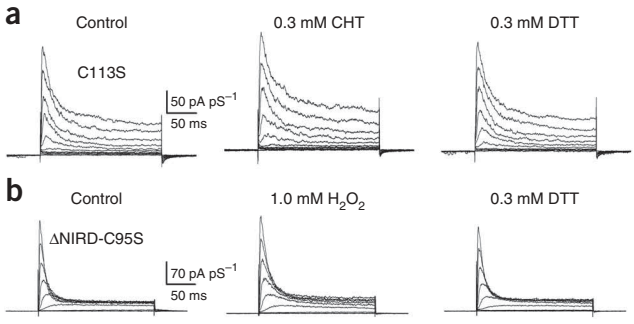

Figure 2 Cys113 mediates redox modulation of KVS-1. (**a**) Representative macroscopic C113S KVS-1 currents elicited by voltage jumps from –80 mV to +120 mV in 20 mV increments (control) and after application of 0.3 mM CHT for 5 min in the test solution, washout, and application of 0.3 mM DTT for 5–10 min in the test solution. (**b**) Representative ΔNIRD-C95S currents (control) and after application of 1 mM H_2O_2 for 2–3 min, washout, and application of 0.3 mM DTT for 5–10 min.

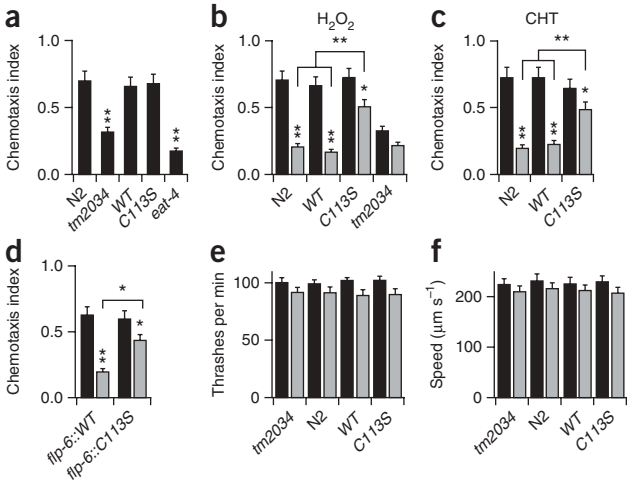

Figure 3 Protected chemosensory function in C113S worms. (**a**) Chemotaxis to biotin in N2 (parental control strain), *tm2034* (*kvs-1* null), *wild type-KVS-1* (*WT*), *C113S-KVS-1* (*C113S*), and chemotaxis-defective *eat-4(ky5)* (ref. 17) larval stage 4 worms; $n = 4$ experiments. (**b**) Chemotaxis of young adult worms to biotin, after soaking in M9 buffer plus 1 mM H_2O_2 in (gray) or M9 buffer alone (black) for 20 min, then 30 min recovery[25] and transfer to a test plate. For N2, *wild type-KVS-1* and *C113S-KVS-1*, $n = 5$ experiments; for *kvs-1* knockout, $n = 3$ experiments. (**c**) As in **b**, but for worms exposed to 0.5 mM CHT for 40 min; $n = 5$ experiments. (**d**) As in **b** but for $P_{flp\text{-}6}$*::wild type-KVS-1* and $P_{flp\text{-}6}$*::C113S-KVS-1* worms; $n = 4$ experiments. (**e**) Forward movement phenotype in the indicated genotypes in control (black) and after exposure to 1 mM H_2O_2 (gray); $n \geq 11$ worms per bar. (**f**) Mean average speeds in the indicated genotypes in control (black) and after exposure to 1 mM H_2O_2 (gray); $n \geq 10$ worms per bar. Mean ± s.e.m.; $^*0.01 < P < 0.05$, $^{**}P < 0.01$.

alterations in these parameters would not necessarily reflect specific defects in spontaneous locomotion). Consistent with the observation that chemotaxis was normal in the $P_{flp\text{-}6}$*::wild type-KVS-1* and $P_{flp\text{-}6}$*::C113S-KVS-1* genotypes, both thrashing and average speed were also normal in *kvs-1* knockout worms (**Fig. 3e,f**). Moreover, thrashing and average speeds in the *wild type-KVS-1* and *C113S-KVS-1* genotypes recapitulated those in the Bristol N2 wild-type strain and, most importantly, treatment with H_2O_2 did not cause a significant loss of locomotor function and affected all genotypes to the same extent (on average, 10%). Together, these data suggest that the improved chemotactic response in *C113S-KVS-1* worms as well as the defective chemotaxis in *kvs-1* null worms is due to the specific contribution of this channel to ASE function rather than to an effect on motor neurons and locomotion. The fact that locomotion is normal in the *kvs-1* null genotype is probably a consequence of compensatory mechanisms that become activated when the expression of KVS-1 is suppressed.

Since ROS levels are thought to increase during aging, we speculated that the chemotactic response should decline in old worms because of KVS-1 oxidation and, therefore, that C113S should attenuate this decline. Indeed, whereas aging worms gradually lost the ability to perform chemotaxis to biotin (75% loss of function in 12 d), the C113S mutation significantly lessened this decline (40% loss, **Fig. 4a**). Similar results were observed for chemotaxis to lysine (70% versus 45%, $n = 3$; data not shown). If oxidation of KVS-1 by ROS were responsible for the loss of chemosensory function associated with aging, chemotaxis would be predicted to be preserved under conditions of low oxidative stress. We therefore used the long-living *age-1(hx546)* mutant worm (TJ1052 strain)[22], which shows higher than wild-type levels of catalase and superoxide dismutase (SOD) activity[23–25] (**Fig. 4**), as a positive control. Accordingly, in *age-1(hx546)* worms, loss of function was marginal and even less pronounced than in *C113S-KVS-1* worms, an effect probably due to the fact that in *age-1(hx546)* neurons many proteins besides KVS-1—including the receptors for biotin—are protected from the effects of ROS.

To further test the hypothesis that loss in chemosensory function in aging worms was caused in part by oxidation of KVS-1, we treated them with DTT. Pre-incubation with DTT yielded a significant gain of function in N2 or *wild type-KVS-1* worms (100%), whereas in *C113S-KVS-1* worms improvement was moderate (15%; **Fig. 4b**). Furthermore, DTT did not significantly rescue the defective chemotactic response of *kvs-1* knockout worms (chemotaxis index, C.I. = 0.17 ± 0.02 and 0.22 ± 0.03 in the absence and presence of DTT, respectively; $n = 2$ experiments). To rule out the possibility that the chemotactic response of *C113S-KVS-1* worms might have been caused

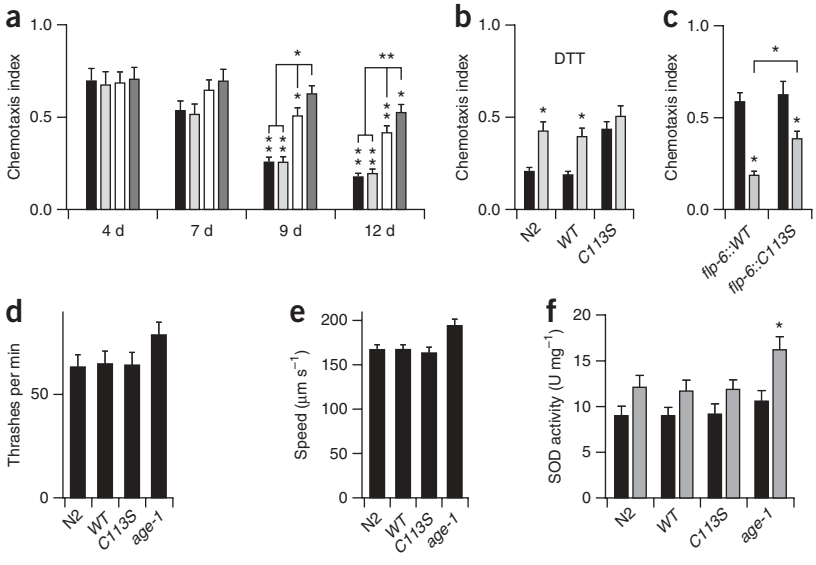

Figure 4 Chemosensory loss is lessened in C113S worms during aging. (**a**) Chemotaxis to biotin in the indicated genotypes (N2, black; *wild type-KVS-1* (*WT*), light gray; *C113S-KVS-1*, white; *age-1(hx546)*, dark gray) at the indicated time points at 20 °C. An experiment started with 600–1,000 age-synchronized worms per genotype, scored for chemotaxis at the indicated time points (~100 worms per time point). N2, *wild type-KVS-1* and *C113S-KVS-1*, $n = 8$ experiments; *age-1(hx546)*, $n = 3$ experiments. (**b**) Chemotaxis of 12-d-old worms to biotin, after soaking in M9 buffer plus 1 mM DTT (gray) or M9 buffer alone (black) for 30 min, then 1–2 h recover and transfer to a test plate; $n = 3$ experiments. (**c**) Chemotaxis to biotin in 4-d-old (black) and 12-d-old (gray) $P_{flp\text{-}6}$*::wild type-KVS-1* and $P_{flp\text{-}6}$*::C113S-KVS-1* worms; $n = 3$ experiments. (**d**) Forward movement phenotype in the indicated genotypes in 12-d-old worms; $n \geq 11$ worms per bar. (**e**) Mean average speed in the indicated genotypes in 12-d-old worms; $n \geq 10$ worms per bar. (**f**) SOD activity in 4-d-old (black) and 12-d-old (gray) worms. SOD activity was normalized to the total protein content of the lysate. $n = 3$ experiments. Mean ± s.e.m.; $^*0.01 < P < 0.05$, $^{**}P < 0.01$.

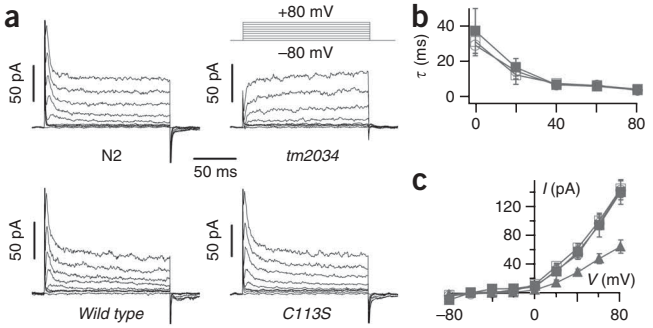

Figure 5 KVS-1 conducts the A-type current in ASER neurons. (**a**) Representative whole-cell currents elicited by voltage jumps from –80 mV to +80 mV (inset) in N2, *wild type-KVS-1*, *C113S-KVS-1* and *tm2034* ASER neurons 4 d after seeding. (**b**) Inactivation rates of currents in N2 (open squares), *wild type-KVS-1* (filled squares) and *C113S-KVS-1* (open circles) neurons. Time constants were calculated by fitting macroscopic currents to a single exponential function (**Supplementary Table 1**); $n = 38$, 13 and 25 cells for, respectively, N2, *wild type-KVS-1* and *C113S-KVS-1*. (**c**) Peak current–voltage relationships in ASER neurons of N2, *wild type-KVS-1*, *C113S-KVS-1* worms and steady-state current-voltage relationship in ASER neurons of *tm2034* worms (triangles); $n = 38$, 13, 25 and 23 cells for, respectively, N2, *wild type-KVS-1*, *C113S-KVS-1* and *tm2034*. ASER neurons were marked by the *Pgcy-5::gfp* reporter, which specifically expresses in this neuron type[15]. Mean ± s.e.m.

by preserved locomotion, we compared chemotaxis in 4- and 12-d-old $P_{flp\text{-}6}$*::wild type-KVS-1* and $P_{flp\text{-}6}$*::C113S-KVS-1* worms (**Fig. 4c**) and counted thrashes and computed mean average speeds as done before (**Fig. 4d**,**e**). As expected, primary expression of C113S KVS-1 in the ASE neurons attenuated the age-related decline in chemosensory function (**Fig. 4c**). Furthermore, loss of locomotor function was similar in old N2, *wild type-KVS-1* and *C113S-KVS-1* worms, and moderate when compared to the decline in chemosensory function (25% versus 75%). This indicates that changes in spontaneous locomotion only marginally affected the decline in chemotaxis during aging in these genotypes. The most likely explanation for the more modest loss of locomotor function in *age-1(hx546)* worms, is retarded muscle sarcopenia[26], an effect that might have contributed to the improved chemotactic response of this mutant.

To eliminate the possibility that differences in anti-oxidant defenses were causative in the enhanced chemotactic response in *C113S-KVS-1* worms, we measured the activity of SOD in 4- and 12-d-old worms. As expected, SOD activity was comparable in all genotypes and augmented in old worms (**Fig. 4f**). This latter observation is consistent with the notion that ROS levels were higher in old worms as it is thought that an increase in SOD activity reflects the response of the organism to oxidative stress in *C. elegans* as well as in mammals including *Homo sapiens*[27,28].

Oxidizing agents modify native KVS-1 channels

To gain insight into the molecular mechanisms underlying the effects of ROS on chemosensory function we characterized the electrophysiology of native cells prepared from embryos, as morphological, electrophysiological, and GFP reporter studies have demonstrated that the differentiation and functional properties of cultured cells are similar to those observed *in vivo*[29–31]. We recorded currents in the ASE right (ASER) neuron because this type of cell is the primary mediator of chemotaxis to water-soluble attractants[32]. Most currents recorded in N2 cells (95%, $n = 38$) 4 d after seeding (**Fig. 5a**) showed robust, voltage-dependent A-type currents that recapitulated native currents present in dissected ASER neurons[14]. Substitution of *N*-methyl-D-glucamine for K^+ in the pipette solution abolished outward currents (data not shown), suggesting that they were carried by K^+ ions. Inactivation was voltage dependent and rapid in N2 neurons (**Fig. 5b**). In contrast, currents in neurons from *tm2034* worms ($n = 23$, **Fig. 5a**) did not inactivate (aside from two cells showing a small inactivating current), were ~50% smaller (**Fig. 5c**) and activated at more positive voltages (**Supplementary Table 2** online). Consistent with the normal chemotaxis seen in *wild type-KVS-1* and *C113S-KVS-1* worms, the currents in neurons from these worms fully recapitulated the currents in N2 neurons (**Fig. 5** and **Supplementary Table 2**) suggesting that little if any overexpression of KVS-1 occurred in the transgenic worms. Taken together, these data indicated that KVS-1 conducts the A-type current in ASER neurons in agreement with previous data obtained with *kvs-1* RNAi[33]. However, heterologously expressed KVS-1 channels, alone or with the accessory subunit MPS-1[10], did not completely recapitulate native channels. There was a –20 mV shift in the $V_{1/2}$ of native currents compared to heterologously expressed currents and the kinetics of inactivation were ~2-fold faster in native than in mammalian cells[10] (**Supplementary Tables 1** and **2**). We do not have a definitive explanation for these discrepancies, but they may reflect differences in plasma membrane composition, the presence of unidentified subunits in native complexes, or lack of the NIRD. We contend these differences are post-translational in origin because *wild type-KVS-1* and *C113S-KVS-1* worms show currents with native attributes. We found another discrepancy between the attributes of heterologously expressed and native KVS-1 channels. Recently, it has been shown that KVS-1 shows cumulative activation when expressed in *Xenopus laevis* oocytes but not in mammalian cells[34]. We tested whether native currents showed cumulative activation but did not observe this phenomenon *in vivo* (data not shown). This suggests that cumulative activation is an effect dependent on the *Xenopus laevis* expression system.

The fact that KVS-1 conducts the A-type current in ASER suggests that native currents are susceptible to oxidation. As expected, application of H_2O_2 in the bath solution quickly converted inactivating currents—in 4-d-old neurons—into non-inactivating currents (**Fig. 6a**). As a consequence of the slowed inactivation of KVS-1, the magnitude of the steady-state current markedly increased. Thus, the fractional current, obtained by dividing the current at the end of the test pulse by the peak current (if the current inactivated) or by the current 5 ms after the beginning of the test pulse (if the current did not inactivate), $I_{steady}/I_{beginning}$, increased from 0.55 ± 0.02 (control) to 1.04 ± 0.07 (after exposure to H_2O_2, $n = 3$ cells; **Fig. 6a**). For quantitative analysis, we recorded currents in the presence of oxidizing agents in the pipette solution. Thus, in N2 and *wild type-KVS-1*, adding H_2O_2 or CHT to the pipette solution suppressed inactivation and resulted in a twofold increase in the fractional current (**Fig. 6b**). Neither H_2O_2 nor CHT significantly altered the currents in *C113S-KVS-1* ASER neurons (**Fig. 6b**). Furthermore, H_2O_2 did not modify the *tm2034* current (**Supplementary Fig. 1** online), indicating that the KVS-1 current is the only component of the ASER K^+ current susceptible to redox modulation.

Endogenous ROS modify native KVS-1 channels

The susceptibility of native currents to oxidizing agents argues that endogenous ROS may cause substantial electrical remodeling in native cells by acting to oxidize KVS-1 channels during aging. In this case, old neurons should show non-inactivating K^+ currents, similar to those in young neurons exposed to oxidizing agents. In fact, the percentage of N2 ASER neurons showing fast-inactivating currents (fractional

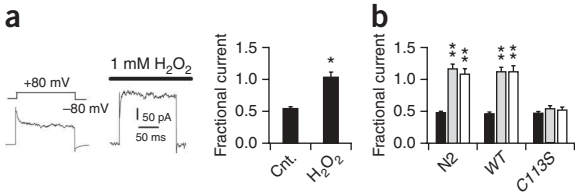

Figure 6 Native KVS-1 currents are modified by oxidizing agents. (**a**) Representative whole-cell currents evoked in a 4-d-old N2 ASER neuron by single voltage jumps from –80 mV to +80 mV (inset) before and after application of 1 mM H_2O_2 in the bath solution. Right, fractional current, $I_{steady}/I_{beginning}$, at +80 mV before (Cnt.) and after exposure to 1 mM H_2O_2; $n = 3$ cells. (**b**) Fractional currents at +80 mV in 4-d-old N2, *wild type-KVS-1* (*WT*) and *C113S-KVS-1* neurons in the absence (black, $n = 15$, 14 and 11 cells, respectively) and presence of 0.25 mM H_2O_2 (gray, $n = 12$, 11 and 9 cells respectively) or 0.25 mM CHT (white, $n = 10$, 11 and 5 cells, respectively) in the patch pipette. Mean ± s.e.m.; *$0.01 < P < 0.05$, **$P < 0.01$.

current < 0.75), which was 95% at day 4, decreased to 41% ($P < 0.0001$) at day 12. The majority of these old neurons (59%; **Fig. 7a**) showed non-inactivating currents. The functional properties of these non-inactivating currents are listed in **Supplementary Table 2**. The slowing of inactivation led to a significant increase in the magnitude of the steady-state current (**Fig. 7a**), an effect that has potentially relevant physiological consequences (see below) and that was reflected in the doubling of the mean fractional current (**Fig. 7b**), without affecting other gating properties such as the voltage dependence of activation (**Supplementary Table 2**). Furthermore, non-inactivating currents were also present in 12-d-old *wild type-KVS-1* ASER neurons in percentages similar to those in N2 cells (54%, compared to 8% at day 4, $P < 0.0001$; **Fig. 7a**,**b** and **Supplementary Table 2**). In contrast, both *C113S-KVS-1* and *age-1(hx546)* neurons seldom showed non-inactivating currents (from 4% at day 4 to 17% at day 12 in *C113S-KVS-1*; from 7% to 20% in *age-1(hx546)*), nor did their mean fractional currents change appreciably during aging (**Fig. 7a**,**b**). Neither were currents in 12-d-old *tm2034* neurons substantially modified (**Supplementary Fig. 1** and **Supplementary Table 2**). To corroborate the notion that in old neurons the modifications in the KVS-1 current were caused by oxidation of KVS-1—presumably by endogenous ROS—we recorded in the absence or presence of DTT. In 12-d-old N2 neurons, application of 0.3 mM DTT in the bath solution (**Fig. 7c**) restored inactivation. Moreover, when DTT was present in the pipette solution, the number of fast-inactivating currents (fractional current < 0.75) rose markedly (**Fig. 7d**) in both N2 (from 43% to 100%; $P < 0.0001$) and *wild type-KVS-1* (from 42% to 92%; $P < 0.0001$) neurons.

To determine how oxidation of KVS-1 affected ASER neuron electrical signaling, we recorded potentials evoked in these cells by current injections. To correlate the oxidation status of KVS-1 with the voltage response of the neuron, we recorded the potentials and the whole-cell currents in the same cell. We examined exemplar potentials elicited in a 4-d-old N2 ASER neuron in response to current injections from –4 pA to +20 pA in 4 pA increments and the corresponding whole-cell currents, recorded immediately after the potentials (**Fig. 7e**). Depolarization was graded with stimulus amplitude and saturated at +78 mV from a resting potential of –55 mV. These voltage responses were markedly nonlinear. The cell depolarized quickly up to roughly 0 mV. Above this threshold, the neuron depolarized considerably more slowly, giving rise to a characteristic biphasic response. These voltage responses recapitulated the potentials recorded in native ASER neurons[14], thereby further validating the use of cultured neurons for electrophysiological studies. As expected, the voltage responses in 12-d-old neurons (**Fig. 7f**), expressing non-inactivating currents (inset), or in 4-d-old neurons recorded in the presence of 0.25 mM

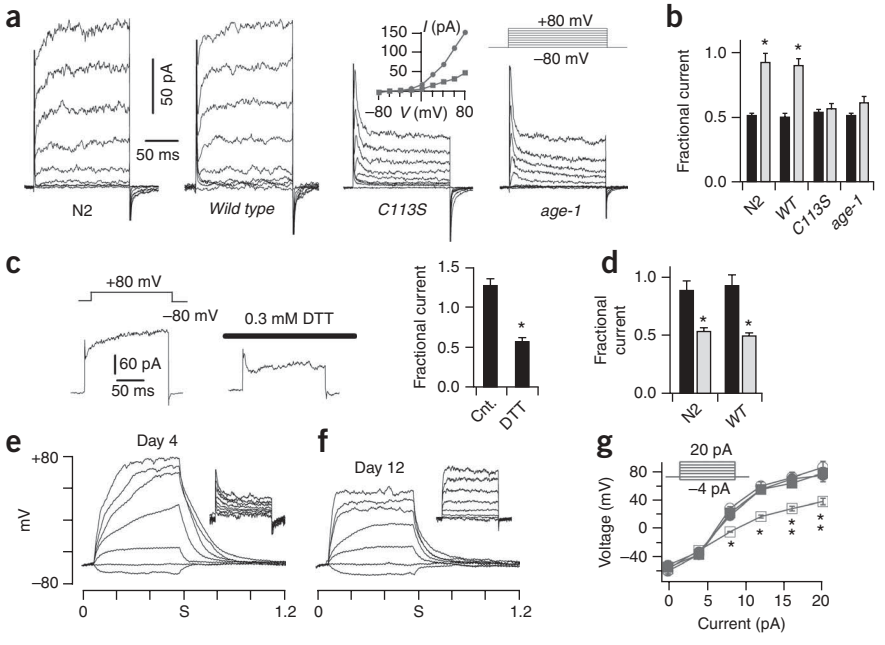

Figure 7 Native KVS-1 currents are modified by endogenous ROS. (**a**) Representative whole-cell currents elicited by single voltage jumps from –80 mV to +80 mV (inset) in a 12-d-old N2, *wild type-KVS-1* (*WT*), *C113S-KVS-1* (*C113S*) and *age-1(hx546)* ASER neuron. Inset, representative steady-state current-voltage relationships in 12-d-old N2 (squares) and *C113S-KVS-1* (circles) cells. (**b**) Mean fractional current at +80 mV, in 4-d-old (black) and 12-d-old (gray) neurons in the N2, *wild type-KVS-1* (*WT*), *C113S-KVS-1* and *age-1(hx546)* genotypes; $n = 38$, 13, 25 and 15 cells, respectively, at day 4 and $n = 29$, 24, 23 and 15 cells, respectively, at day 12. (**c**) Representative whole-cell currents evoked in an N2 ASER neuron by single voltage jumps from –80 mV to +80 mV (inset) before and after application of 0.3 mM DTT in the bath solution. Right, fractional current at +80 mV before (Cnt.) and after exposure to DTT, $n = 3$ cells. (**d**) Mean fractional current in 12-d-old N2 or *wild type-KVS-1* neurons recorded in the absence (black, $n = 21$ and 19 cells, respectively) or presence of 0.2 mM DTT in the pipette solution (gray, $n = 12$ and 13 cells, respectively). (**e**) Representative potentials evoked in a 4-d-old N2 ASER cultured neuron in response to 0.5 s current injections from –4 pA to 20 pA in 4 pA increments (current protocol in the inset of **Fig. 7f**). Inset, whole-cell currents recorded in the same cell evoked by 1-s voltage steps from –80 mV to +80 mV in 20 mV increments. (**f**) As in **e** but in a 12-d-old N2 ASER neuron. (**g**) Steady-state voltage–current relationships in 4-d-old N2 neurons (filled squares; fractional current 0.49 ± 0.08, $n = 8$ cells), 12-d-old N2 neurons (open squares; fractional current 0.98 ± 0.07, $n = 7$ cells), 4-d-old *C113S-KVS-1* neurons (filled circles; fractional current 0.50 ± 0.04, $n = 6$ cells) and 12-d-old *C113S-KVS-1* neurons (hollow circles; fractional current 0.43 ± 0.04, $n = 7$ cells). Mean ± s.e.m.; *$0.01 < P < 0.05$, **$P < 0.01$.

Table 1 Electrophysiological properties of native ASER potentials

Genotype		V_{12} (mV)	t_{r12} (s)	*n*
N2	Day 4	55 ± 5.5	0.33 ± 0.03	8
	Day 12	17 ± 2.0*	0.08 ± 0.01**	7
	H_2O_2	14 ± 1.0**	0.09 ± 0.01**	5
C113S	Day 4	55 ± 6.6	0.30 ± 0.4	6
	Day 12	60 ± 6.0	0.35 ± 0.4	7
	H_2O_2	57 ± 6.1	0.28 ± 0.3	5
tm2034	Day 4	59 ± 5.8	0.08 ± 0.01**	5
	Day 12	57 ± 6.3	0.07 ± 0.01*	4

V_{12} and t_{r12} indicate the steady-state potential and the time necessary to reach 90% of steady-state value attained by the cell in response to a current injection of 12 pA. Data are presented as mean ± s.e.m.; *$0.01 < P < 0.05$, **$P < 0.01$.

H_2O_2 in the patch pipette (**Table 1**), were markedly different. First, the maximum depolarization attained by old cells at steady-state was significantly lower (38 mV, **Fig. 7g**; see also **Table 1**). Second, the cell depolarized significantly faster (fourfold), without the characteristic biphasic kinetics (**Fig. 7f** and **Table 1**). Rise times in 4- and 12-d-old *kvs-1* null neurons were also significantly faster and monophasic than those in N2 neurons (**Table 1** and **Supplementary Fig. 1**), indicating that under normal conditions, the A-type current conducted by KVS-1 is responsible for the kinetics of activation of the ASER voltage response. Because the current in ASER neurons expressing C113S KVS-1 does not appreciably change during aging or in the presence of oxidizing agents, the voltage responses in this genotype should also not change. As expected, the potentials elicited in *C113S KVS-1* ASERs recapitulated those in N2 neurons at day 4 and did not significantly change during aging (**Fig. 7g**) nor in the presence of H_2O_2 (**Table 1**). Together these data establish a direct link between oxidative regulation of KVS-1 function during aging and ASER neuron signaling.

In summary, both the resistance of KVS-1 to oxidation (conferred by the C113S mutation) and the increased antioxidant defenses in *age-1(hx546)* acted to prevent modification of the ASER K^+ current by ROS during aging and, as a consequence, modification of ASER excitability. These findings indicate that primary ASER neurons are subject to normal aging processes, even though the amounts of ROS in cultured neurons and *in vivo* may be different. We conclude that oxidation of KVS-1 by ROS represents a substantial cause of electrical remodeling in the ASE neurons, a fact that provides a natural explanation for the progressive loss in chemosensory function in the worm during aging.

DISCUSSION

To answer fundamental questions about the role played by physiological interactions of ROS with K^+ channels in regulating neuronal function, we developed a *C. elegans* animal model of K^+ channel–mediated protection from oxidative stress using voltage-gated K^+ channel KVS-1 and a redox-resistant variant, C113S. We found that altered neuronal excitability, through ROS-mediated modification of KVS-1, is a significant cause of sensorial decline during aging in *C. elegans*. Thus, chemotaxis to biotin and lysine—a sensory function controlled by KVS-1—progressively declined in aging worms. This loss was mimicked by exposing young worms to oxidizing agents and reversed by treating old worms with DTT. By contrast, loss of chemosensory function was significantly lessened in worms harboring the C113S variant (even though their SOD levels were not different) and in *age-1(hx546)* worms, which overexpress antioxidant defenses. Because we measured the activity of SOD in the entire organism, we cannot rule out the possibility that SOD levels changed only in the neurons expressing KVS-1, although this seems very unlikely. Electrophysiological analyses showed that the native potassium current in the ASER neuron, a cell that mediates chemotaxis to biotin and lysine, was altered by both endogenous and exogenous ROS through specific modification of KVS-1 channels, whereas in neurons expressing C113S, or in conditions of low oxidative stress in the *age-1(hx546)* genotype, the current was modified very little. As expected, oxidative modifications in the KVS-1 current had a profound impact on ASER excitability by acting to alter both the transient and steady-state characteristics of its voltage responses.

The effects of oxidation of KVS-1 were most easily noticed at voltages that generally are outside the physiological range of vertebrate cells. However, it seems to be a common property of *C. elegans* neurons and muscles to work at more positive voltages than the cells of other species; consequently, potassium channels activate at more depolarizing voltages than their mammalian homologs[14,35–40]. Our data showed that the ASER neuron was extremely responsive to input currents; currents of few picoamps could depolarize this cell by tens of millivolts. Thus, the opening of a few receptor channels, in the physiological range, can significantly depolarize this cell. In conclusion, these data show that KVS-1 conducts a current that has a profound impact on the signaling ability of the ASER. A detailed investigation of the mechanisms by which KVS-1 shapes ASER neuron signaling are beyond the scope of this study and will be the subject of a future study.

Although our data underscore a prominent role of Cys113 in the molecular mechanism by which redox modifications slow KVS-1 inactivation, it remains to be determined whether oxidation of this residue leads to formation of disulfide-bonded cysteines (between two Cys113 residues or, alternatively, with a cysteine in the Cys172-Cys173 pair) or, alternatively, sulfinic or sulfonic acid. Residues other than cysteines, methionines for example, are not likely to play a role because they would not be reduced by DTT[41]. Further investigations will address this issue.

Evidence has been accumulating that aging in mammalian neurons is associated with changes in K^+ homeostasis[42,43]. In particular, cortical neurons deficient in Kv2.1 channels (a KVS-1 homolog) are protected from oxidant-induced apoptosis *in vitro*[44]. The elevation of ROS in the aging brain[45], and the ROS-induced neurodegeneration seen in many neuronal pathologies including Alzheimer's disease[46] and multiple sclerosis[47], prompts the idea that the chain of events leading to age-related neurodegeneration in the nervous system of mammals could involve the interaction of ROS with K^+ channels. Thus, oxidative modification of K^+ channels might represent a fundamental pathogenic mechanism in mammals.

In summary, we report a simple physiological process through which voltage-gated K^+ channels lead to sensorial decline during aging. Considering that K^+ channels and ROS are universal players in the biological game, we put forward the idea that physiological oxidation of voltage-gated K^+ channels may represent a common pathogenic mechanism in biological organisms.

METHODS

Strains. We used strains Bristol (N2), tm2034, age-1(hx546), eat-4(ky5), tm2034(P_{KVS-1}::KVS-1)(myo-2::gfp) (termed wild type-KVS-1), tm2034(P_{KVS-1}::C113S-KVS-1)(myo-2::gfp) (termed C113S-KVS-1), tm2034(P_{KVS-1}::KVS-1)(myo-2::gfp)(gcy-5::gfp)(rol-6), tm2034(P_{KVS-1}::C113S-KVS-1)(myo-2::gfp)(gcy-5::gfp)(rol-6), age-1(hx546)(gcy-5::gfp)(rol-6), tm2034(Pf_{lp-6}::KVS-1)(myo-2::gfp)(gcy-5::gfp) and tm2034(Pf_{lp-6}::C113S)(myo-2::gfp)(gcy-5::gfp).

Strain construction. A 3,162-bp fragment (termed the promoter of *kvs-1* or P_{kvs-1}) was amplified by PCR from the C53C9 cosmid and subcloned in the

pPD95.75 Fire vector ($P_{kvs\text{-}1}$*::gfp* construct) alone or with the cDNA encoding KVS-1 (*wild type-KVS-1*) or its C113S mutant (*C113S-KVS-1*). Transformant lines for *wild type-KVS-1* and *C113S-KVS-1* were integrated by γ-irradiation (4,000 rad for 40 min). $P_{kvs\text{-}1}$*::gfp* yielded GFP signals in several amphid neurons, including the ASEs, ventral cord motor neurons, and those of the vulva and anal depressor muscle[10] (**Supplementary Fig. 2** online). We amplified 2,481 bp of genomic DNA (termed the promoter of *flp-6*, or $P_{flp\text{-}6}$) by PCR and subcloned it in a construct containing the cDNA encoding KVS-1 ($P_{flp\text{-}6}$*::wild type-KVS-1*) or C113S KVS-1 ($P_{flp\text{-}6}$*::C113S-KVS-1*) in the pPD95.75 vector.

We performed behavioral tests as described previously[10], without knowledge of the worms' genotype. Aging experiments started with ~600–1,000 age-synchronized worms per genotype (except with *Pflp-6::wild type-KVS-1* and *Pflp-6::C113S-KVS-1*, which started with ~200–300 age-synchronized worms). We examined worms every day until death and scored them as dead when they no longer moved even in response to prodding with a platinum pick. Quantitative data are presented as mean ± s.e.m.

Additional methods. Full methods and any associated references are available in the **Supplementary Methods** online.

Note: Supplementary information is available on the Nature Neuroscience website.

ACKNOWLEDGMENTS

We thank S. Mitani (Tokyo Women's Medical University School of Medicine) for the *tm2034* strain, O. Hobert (Columbia University) for the *Pgcy-5::GFP* construct and the *C. elegans* Knockout Consortium for the TJ1052 strain. We thank A. Jauregui and M. Barr for their help with the average speed measurements, and J. Lenard, G. Abbott and L. Runnels for critical reading of the manuscript. This work was supported by a US National Institutes of Health grant (R01GM68581) to F.S.

AUTHOR CONTRIBUTIONS

S.-Q.C. and F.S. designed research, performed research and analyzed data. F.S. wrote the manuscript.

Published online at http://www.nature.com/natureneuroscience/
Reprints and permissions information is available online at http://npg.nature.com/reprintsandpermissions/

1. Harman, D. Aging: a theory based on free radical and radiation chemistry. *J. Gerontol.* **11**, 298–300 (1956).
2. Annunziato, L. *et al.* Modulation of ion channels by reactive oxygen and nitrogen species: a pathophysiological role in brain aging? *Neurobiol. Aging* **23**, 819–834 (2002).
3. Ruppersberg, J.P. *et al.* Regulation of fast inactivation of cloned mammalian IK(A) channels by cysteine oxidation. *Nature* **352**, 711–714 (1991).
4. Duprat, F., Girard, C., Jarretou, G. & Lazdunski, M. Pancreatic two P domain K+ channels TALK-1 and TALK-2 are activated by nitric oxide and reactive oxygen species. *J. Physiol. (Lond.)* **562**, 235–244 (2005).
5. Tang, X.D., Garcia, M.L., Heinemann, S.H. & Hoshi, T. Reactive oxygen species impair Slo1 BK channel function by altering cysteine-mediated calcium sensing. *Nat. Struct. Mol. Biol.* **11**, 171–178 (2004).
6. Zeidner, G., Sadja, R. & Reuveny, E. Redox-dependent gating of G protein-coupled inwardly rectifying K+ channels. *J. Biol. Chem.* **276**, 35564–35570 (2001).
7. Avshalumov, M.V. & Rice, M.E. Activation of ATP-sensitive K+ (K(ATP)) channels by H2O2 underlies glutamate-dependent inhibition of striatal dopamine release. *Proc. Natl. Acad. Sci. USA* **100**, 11729–11734 (2003).
8. Gamper, N. *et al.* Oxidative modification of M-type K(+) channels as a mechanism of cytoprotective neuronal silencing. *EMBO J.* **25**, 4996–5004 (2006).
9. Kenyon, C. (ed.) *Environmental factors and gene activities that influence life span.* (Cold Spring Harbor Laboratory Press, Cold Spring Harbor, 1997).
10. Bianchi, L., Kwok, S.M., Driscoll, M. & Sesti, F. A potassium channel-MiRP complex controls neurosensory function in *Caenorhabditis elegans*. *J. Biol. Chem.* **278**, 12415–12424 (2003).
11. Cai, S.Q. & Sesti, F. A new mode of regulation of N-type inactivation in a *Caenorhabditis elegans* voltage-gated potassium channel. *J. Biol. Chem.* **282**, 18597–18601 (2007).
12. Hoshi, T., Zagotta, W.N. & Aldrich, R.W. Biophysical and molecular mechanisms of Shaker potassium channel inactivation. *Science* **250**, 533–538 (1990).
13. Bargmann, C. & Mori, I. in *C. elegans II* (eds. Riddle, D.L., Blumenthal, B.T, Meyer, B.J. & Priess, J.R.) 717–737 (Cold Spring Harbor Laboratory Press, Cold Spring Harbor, New York, USA, 1997).
14. Goodman, M.B., Hall, D.H., Avery, L. & Lockery, S.R. Active currents regulate sensitivity and dynamic range in *C. elegans* neurons. *Neuron* **20**, 763–772 (1998).
15. Yu, S., Avery, L., Baude, E. & Garbers, D. Guanylyl cyclase expression in specific sensory neurons: a new family of chemosensory receptors. *Proc. Natl. Acad. Sci. USA* **94**, 3384–3387 (1997).
16. Kim, K. & Li, C. Expression and regulation of an FMRFamide related neuropeptide gene family in *Caenorhabditis elegans*. *J. Comp. Neurol.* **475**, 540–550 (2004).
17. Lee, R.Y., Sawin, E.R., Chalfie, M., Horvitz, H.R. & Avery, L. EAT-4, a homolog of a mammalian sodium-dependent inorganic phosphate cotransporter, is necessary for glutamatergic neurotransmission in *Caenorhabditis elegans*. *J. Neurosci.* **19**, 159–167 (1999).
18. Miller, K.G. *et al.* A genetic selection for *Caenorhabditis elegans* synaptic transmission mutants. *Proc. Natl. Acad. Sci. USA* **93**, 12593–12598 (1996).
19. Ramot, D., Johnson, B.E., Berry, T.L. Jr., Carnell, L. & Goodman, M.B. The Parallel Worm Tracker: a platform for measuring average speed and drug-induced paralysis in nematodes. *PLoS ONE* **3**, e2208 (2008).
20. Pierce-Shimomura, J.T., Morse, T.M. & Lockery, S.R. The fundamental role of pirouettes in *Caenorhabditis elegans* chemotaxis. *J. Neurosci.* **19**, 9557–9569 (1999).
21. Suzuki, H. *et al.* Functional asymmetry in *Caenorhabditis elegans* taste neurons and its computational role in chemotaxis. *Nature* **454**, 114–118 (2008).
22. Klass, M.R. A method for the isolation of longevity mutants in the nematode *Caenorhabditis elegans* and initial results. *Mech. Ageing Dev.* **22**, 279–286 (1983).
23. Lithgow, G.J., White, T.M., Melov, S. & Johnson, T.E. Thermotolerance and extended life-span conferred by single-gene mutations and induced by thermal stress. *Proc. Natl. Acad. Sci. USA* **92**, 7540–7544 (1995).
24. Vanfleteren, J.R. Oxidative stress and ageing in *Caenorhabditis elegans*. *Biochem. J.* **292**, 605–608 (1993).
25. Larsen, P.L. Aging and resistance to oxidative damage in *Caenorhabditis elegans*. *Proc. Natl. Acad. Sci. USA* **90**, 8905–8909 (1993).
26. Herndon, L.A. *et al.* Stochastic and genetic factors influence tissue-specific decline in ageing *C. elegans*. *Nature* **419**, 808–814 (2002).
27. Darr, D. & Fridovich, I. Adaptation to oxidative stress in young, but not in mature or old, *Caenorhabditis elegans*. *Free Radic. Biol. Med.* **18**, 195–201 (1995).
28. Okabe, T., Hamaguchi, K., Inafuku, T. & Hara, M. Aging and superoxide dismutase activity in cerebrospinal fluid. *J. Neurol. Sci.* **141**, 100–104 (1996).
29. Christensen, M. *et al.* A primary culture system for functional analysis of *C. elegans* neurons and muscle cells. *Neuron* **33**, 503–514 (2002).
30. Zhang, Y. *et al.* Identification of genes expressed in *C. elegans* touch receptor neurons. *Nature* **418**, 331–335 (2002).
31. Suzuki, H. *et al.* In vivo imaging of *C. elegans* mechanosensory neurons demonstrates a specific role for the MEC-4 channel in the process of gentle touch sensation. *Neuron* **39**, 1005–1017 (2003).
32. Bargmann, C.I. & Horvitz, H.R. Chemosensory neurons with overlapping functions direct chemotaxis to multiple chemicals in *C. elegans*. *Neuron* **7**, 729–742 (1991).
33. Park, K.H., Hernandez, L., Cai, S.Q., Wang, Y. & Sesti, F. A Family of K+ Channel Ancillary Subunits Regulate Taste Sensitivity in *Caenorhabditis elegans*. *J. Biol. Chem.* **280**, 21893–21899 (2005).
34. Rojas, P. *et al.* Cumulative activation of voltage-dependent KVS-1 potassium channels. *J. Neurosci.* **28**, 757–765 (2008).
35. Santi, C.M. *et al.* Dissection of K+ currents in *Caenorhabditis elegans* muscle cells by genetics and RNA interference. *Proc. Natl. Acad. Sci. USA* **100**, 14391–14396 (2003).
36. Ramot, D., MacInnis, B.L. & Goodman, M.B. Bidirectional temperature-sensing by a single thermosensory neuron in *C. elegans*. *Nat. Neurosci.* **11**, 908–915 (2008).
37. Richmond, J.E. Electrophysiological recordings from the neuromuscular junction of *C. elegans*. in *WormBook* (ed. The *C. elegans* Research Community) 1–8 doi/10.1895/wormbook.1.112.1 (6 October 2006).
38. Jospin, M., Mariol, M., Segalat, L. & Allard, B. Characterization of K^+ currents using an in situ patch-clamp technique in body wall muscle cells from. *Caenorhabditis elegans*. *J. Physiol.* **544**, 373–384 (2002).
39. Richmond, J.E. & Jorgensen, E.M. One GABA and two acetylcholine receptors function at the *C. elegans* neuromuscular junction. *Nat. Neurosci.* **2**, 791–797 (1999).
40. Mellem, J.E., Brockie, P.J., Madsen, D.M. & Maricq, A.V. Action potentials contribute to neuronal signaling in *C. elegans*. *Nat. Neurosci.* **11**, 865–867 (2008).
41. Ciorba, M.A., Heinemann, S.H., Weissbach, H., Brot, N. & Hoshi, T. Modulation of potassium channel function by methionine oxidation and reduction. *Proc. Natl. Acad. Sci. USA* **94**, 9932–9937 (1997).
42. Alshuaib, W.B. *et al.* Reduced potassium currents in old rat CA1 hippocampal neurons. *J. Neurosci. Res.* **63**, 176–184 (2001).
43. Yu, S.P. *et al.* Mediation of neuronal apoptosis by enhancement of outward potassium current. *Science* **278**, 114–117 (1997).
44. Pal, S., Hartnett, K.A., Nerbonne, J.M., Levitan, E.S. & Aizenman, E. Mediation of neuronal apoptosis by Kv2.1-encoded potassium channels. *J. Neurosci.* **23**, 4798–4802 (2003).
45. Serrano, F. & Klann, E. Reactive oxygen species and synaptic plasticity in the aging hippocampus. *Ageing Res. Rev.* **3**, 431–443 (2004).
46. Behl, C. Alzheimer's disease and oxidative stress: implications for novel therapeutic approaches. *Prog. Neurobiol.* **57**, 301–323 (1999).
47. Bo, L. *et al.* Induction of nitric oxide synthase in demyelinating regions of multiple sclerosis brains. *Ann. Neurol.* **36**, 778–786 (1994).

Cai and Sesti

Oxidation of a potassium channel causes progressive sensory function loss during ageing.

SUPPLEMETARY INFORMATION

Table S-1 Electrophysiological properties of ΔNIRD KVS-1 channels in heterologous expression systems (CHO, HEK 293)

	σ_{120} (pA/pF)	τ_{120} (ms)	$V_{1/2}$ (mV)	V_S (mV)	n
ΔNIRD					
Cnt. CHT DTT	210 ± 23 248 ± 29 227 ± 27	11 ± 1.0 88 ± 9.1** 13 ±1.3	47.1 ± 2.1 44.6 ± 2.7 46.9 ± 2.2	19.7 ± 1.1 19.4 ± 1.2 20.6 ± 1.4	9
Cnt. H_2O_2 DTT	273 ± 36 317 ± 51 291 ± 47	9.7 ± 1.0 94 ± 9.6* 16 ±1.7	45.7 ± 2.8 44.3 ± 2.5 47.4 ± 2.8	20.9 ± 1.4 20.2 ± 1.6 19.0 ± 1.6	6
ΔNIRD-C95S					
Cnt. CHT DTT	202 ± 19 200 ± 26 207 ± 25	10 ± 9.4 19 ± 1.8* 11 ± 1.1	46.1 ± 2.2 44.6 ± 1.4 47.7 ± 2.1	20.0 ± 1.3 19.1 ± 1.5 21.2 ± 1.5	8
Cnt. H_2O_2 DTT	289 ± 41 292 ± 48 299 ± 50	9.6 ± 1.0 16 ± 1.9* 13 ± 1.7	45.8 ± 2.4 47.3 ± 2.9 45.5 ± 2.3	21.2 ± 1.8 20.6 ± 1.5 19.9 ± 1.7	6
ΔNIRD+MPS-1					
Cnt. CHT	107 ± 15 111 ± 16	7.4 ± 0.9 94 ± 14*	35.6 ± 2.8 37.4 ± 3.0	20.5 ± 1.6 20.0 ±1.7	5
ΔNIRD-C95S+MPS-1					
Cnt. CHT	124 ± 16 120 ± 18	8.6 ± 1.2 14 ± 2.0	36.1 ± 2.5 35.9 ± 3.2	19.4 ± 1.6 19.5 ± 1.5	5

Currents were elicited by voltage jumps from –80 mV to +120 mV in 20 mV increments. Current densities, σ_{120}, were calculated by normalizing the peak current at +120 mV to the cell capacitance. Time constants at +120 mV, τ_{120}, were calculated by fitting macroscopic currents to a single exponential function:

$$I(t) = I_0 + I_1 e^{-t/\tau} \qquad \text{(S-1)}$$

The half-maximal voltage, $V_{1/2}$ and the slope factor V_s were calculated by fitting macroscopic conductance-V relationships (G) to the Boltzmann equation:

$$G(V) = \frac{I}{V - V_{rev.}} = \frac{G_{Max}}{1 + e^{(V_{1/2} - V)/V_s}} \qquad \text{(S-2)}$$

where I is the macroscopic peak current, V is the applied voltage, and $V_{rev.}$ is the computed Nernst potential for K^+ at the experimental concentrations (–87 mV). CHT and DTT were applied on the same cell (as shown in **Fig. 1**). CHT was supplied for 5 minutes and DTT for 5–10 minutes. H_2O_2 and DTT were applied on the same cell. H_2O_2 was applied for 2–3 minutes and DTT for 5–10 minutes. Wild type KVS-1 channels were expressed in CHO cells. ΔNIRD and ΔNIRD-C95S channels were expressed in CHO cells and in HEK cells. Channels expressed in CHO cells were tested for susceptibility to CHT, channels expressed in HEK cells were tested for susceptibility to H_2O_2.

Statistically significant differences from control are indicated with * ($0.01 < P < 0.05$) and ** ($P < 0.01$).

Table S-2 Electrophysiological properties of native ASER currents				
	I_{80}(pA)	**$V_{1/2}$ (mV)**	**V_S (mV)**	**n**
Day four				
N2.	67 ± 6.1	29.7 ± 1.9	20.7 ± 1.0	38
tm2034	64 ± 9.1	36.3 ± 1.8**	16.0 ± 1.0**	23
Wild type-KVS-1	66 ± 7.5	30.9 ± 2.4	19.9 ± 1.3	13
C113S-KVS-1	62 ± 5.6	30.2 ± 2.2	20.3 ± 1.1	25
age-1(hx546)	65 ± 6.3	30.2 ± 1.9	21.8 ± 1.4	15
Day twelve				
N2	110± 12*	29.8 ± 1.6	20.0 ± 1.5	29
tm2034	61 ± 7.8	37.0 ± 1.9**	15.4 ± 1.1**	14
Wild type-KVS-1	102 ± 12*	30.1 ± 2.3	20.1 ± 1.3	24
C113S-KVS-1	66± 6.0	30.3 ± 2.8	19.8 ± 1.6	23
age-1(hx546)	70 ± 7.3	31.4 ± 2.3	21.1± 2.0	15

Currents were elicited by voltage jumps from –80 mV to +80 mV in 20 mV increments. I_{80} indicates the steady-state current at +80 mV.

The half maximal voltage, $V_{1/2}$ and the slope factor V_s were calculated by fitting macroscopic conductance-V relationships (G) to eqn. (S-2) with $V_{rev.}$ = –89 mV. Statistically significant differences from control are indicated with * ($0.01 < P < 0.05$) and ** ($P < 0.01$).

Figure S-1

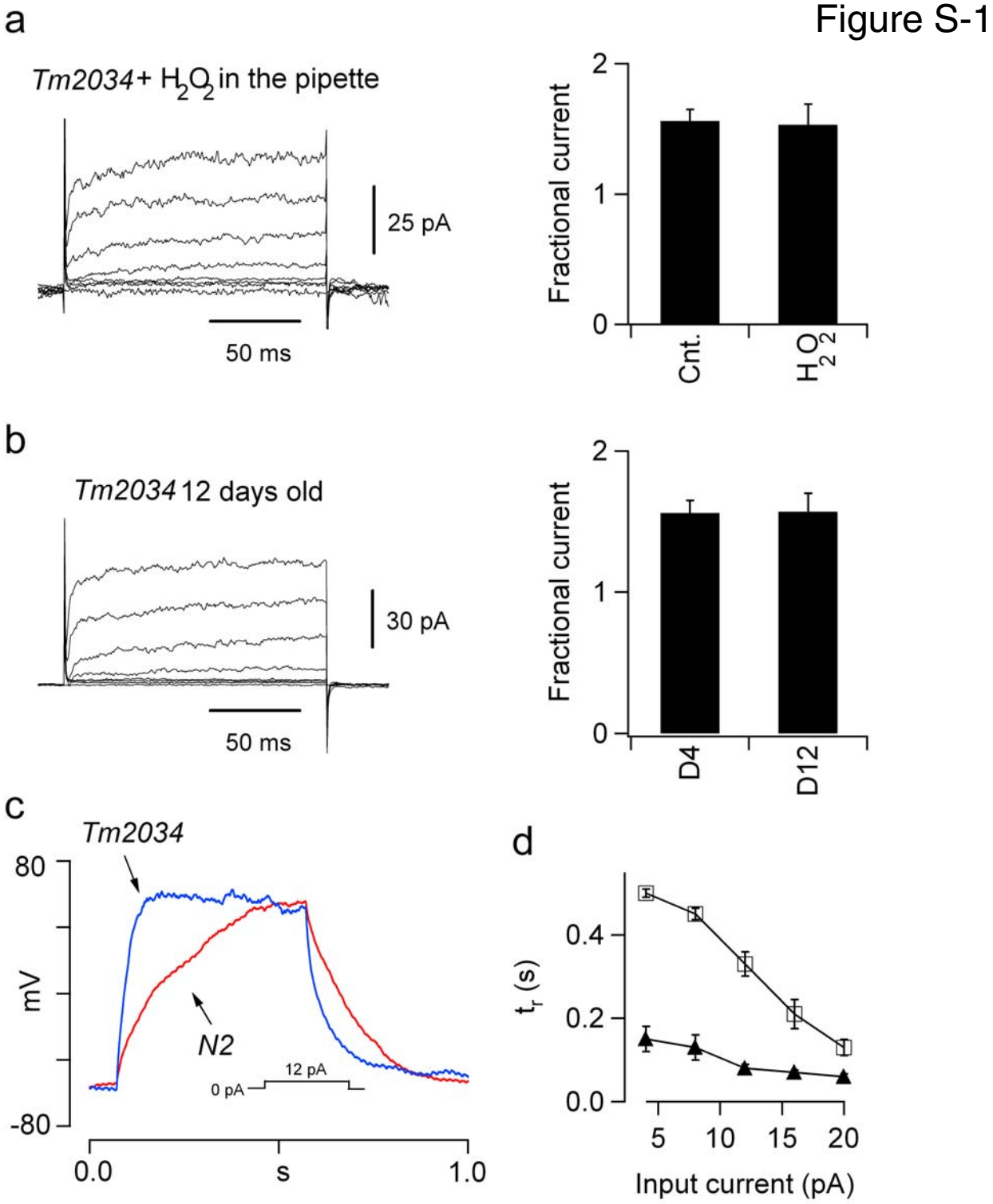

Fig. S-1 (a) Representative whole-cell currents evoked in a four days old N2 *tm2034* ASER neuron by single voltage jumps from -80 mV to +80 mV in the presence of 0.25 mM H2O2 in the pipette. Right, fractional current, in the absence (n = 22) or presence of 0.25 mM H2O2 (n = 7) in the pipette. **(b)** Representative whole-cell currents in a twelve days old N2 *tm2034* ASER neuron. Right, fractional current, in 4 days old (same as in (A)) and 12 days old neurons (n = 14). **(c)** Representative potentials evoked in 4 days old N2 (red) and *tm2034* (blue) ASER cultured neurons in response to a 12 pA current injection. **(d)** Rise times in 4 days old N2 (squares) and *tm2034* (triangles) neurons. n = 8 cells and n = 5 cells for respectively, N2 and *tm2034*.

Nature Neuroscience: doi.10.1038/nn.2291

Figure S-2

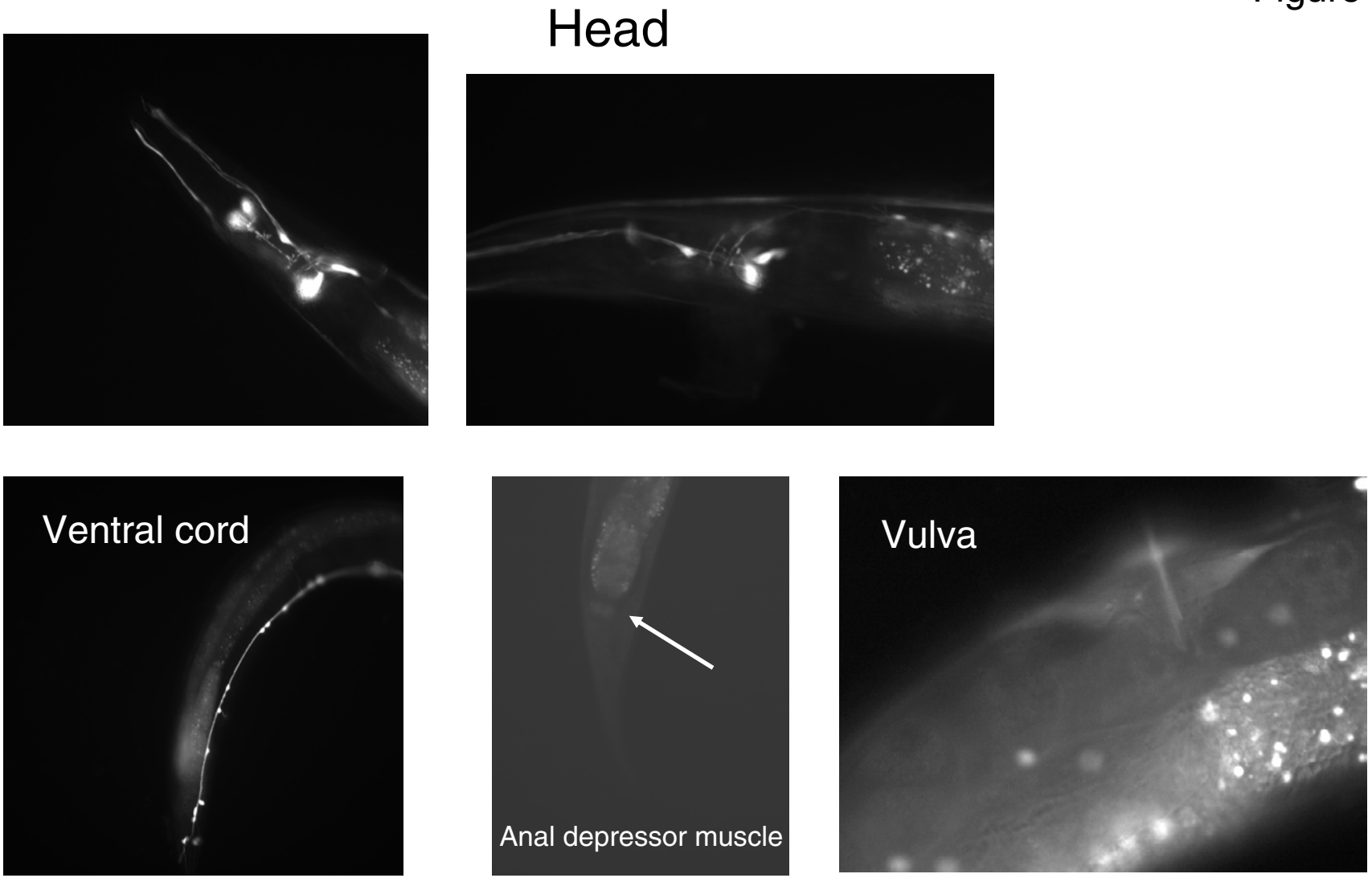

Fig. S-2 Fluorescence microscopy images taken from P*kvs-1::gfp* transgenic nematodes showing GFP signals in neurons of the head including the amphid neurons (in two different focal plans), in the ventral cord neurons, in the anal depressor muscle (arrow) and vulva. Images were taken with an Olympus BX61 microscope equipped with a digital camera.

Nature Neuroscience: doi.10.1038/nn.2291

FULL METHODS

Molecular Biology

Cysteine mutants (C113S, ΔNIRD-C95S, C151S, C2 09S, C283S and C172S-C173S), were constructed by polymerase chain reaction (PCR) using *Pfu* polymerase (Stratagene) and wild-type or ΔNIRD (obtained by deleting the first 18 amino acids, [1]) KVS-1 cDNA in the pCI-neo vector (Promega).

Strains

Strain used were Bristol (*N2*) , *tm2034* (*kvs-1* KO; outcrossed four times) *age-1(hx546)* and *eat-4(ky5).* We constructed: *tm2034(P_{KVS-1}::KVS-1)(myo-2::gfp),* termed *wild-type-KVS-1, tm2034(P_{KVS-1}::C113S-KVS-1)(myo-2::gfp),* termed *C113S-KVS-1*, *tm2034(P_{KVS-1}::KVS-1)(myo-2::gfp)(gcy-5::gfp)(rol-6)*, *tm2034(P_{KVS-1}::C113S-KVS-1)(myo-2::gfp)(gcy-5::gfp)(rol-6)* and *age-1(hx546)(gcy-5::gfp)(rol-6), tm2034(Pf_{lp-6}::KVS-1)(myo-2::gfp)(gcy-5::gfp)* and *tm2034(Pf_{lp-6}::C113S)(myo-2::gfp)(gcy-5::gfp).*

Construction of transgenic animals

The promoter of kvs-1. A 3162 bp fragment of intronic sequence upstream exon 2 (termed the promoter of *kvs-1* or P_{kvs-1}) was amplified by PCR from the C53C9 cosmid and subcloned into the pPD95.75 Fire vector (*P_{kvs-1}::gfp* construct), using BamH I and Xma I restriction sites. Primers: 5'-

CGCGGATCCATGATGCTTCTTCATGAT-3' and 5'-TCCCCCCGGGGGCAATTTGGTTGCTGAA-3'. P_{kvs-1}*::gfp* was injected into the syncitial gonads of adult *tm2034* hermaphrodites. P_{kvs-1}*::gfp* yielded GFP signals in several amphid neurons including the ASEs, vulva, ventral cord motor-neurons and anal depressor muscle [2] (**Fig. S-2)**.

The flp-6 promoter. 2481 bp of genomic DNA (the promoter of *flp-6,* termed P_{flp-6}) were amplified by PCR using the following primers: 5'-AAGCTTACTGCATAAAAAAACAACAAAAAAAAATAA-3' and 5'-CCCGGGATTCTGGAATAATCATATTGTTTTCAAAAT-3' and subcloned in a construct containing wild-type KVS-1 or C113S KVS-1 cDNA in pPD95.75 using Hind III and SAM I restriction sites.

Wild-type-KVS-1 and C113S-KVS-1 transgenic worms For transgenic expression of KVS-1, Xma I and KPN I restriction sites were added by PCR in wild-type and C113S KVS-1 cDNA (5'-TCCCCCCGGGATGAGCACGGAAAGGCTG-3' and 5'-CGGGGTACCAACGATTCTGCCACATCAAT-3') and subcloned in P_{kvs-1} in pPD95.75. The constructs were injected into the syncitial gonads of adult *tm2034* hermaphrodites. Transformant lines for *wild-type-KVS-1* and *C113S-KVS-1* were each stabilized by a mutagenesis-induced integration into a chromosome by irradiating 40 animals with γ-ray with 4000 rads for 40 minutes. The progeny were checked for 100% transmission of the marker (*myo-2::gfp*) and also for the presence of the transgene by PCR amplification. Two lines for *wild-type-KVS-1, tm2034*(P_{KVS-1}*::KVS-1)(myo-2::gfp)* (#3 and #4) and two lines for *C113S-KVS-1, tm2034*(P_{KVS-1}*::C113S-KVS-1)(myo-2::gfp)* (#7 and #11) were outcrossed four

times. These lines gave similar results in chemotaxis assays. The data presented in this study were obtained with lines #3 and #11. For electrophysiology lines #3 and #11 were injected with the *Pgcy-5::gfp* construct. Because these lines express GFP in the pharynx, the transformation marker was *rol-6*. Thus, for electrophysiology, strains used were *tm2034(P_{KVS-1}::KVS-1)(myo-2::gfp)(gcy-5::gfp)(rol-6)*, *tm2034(P_{KVS-1}::C113S-KVS-1)(myo-2::gfp)(gcy-5::gfp)(rol-6)* and *age-1(hx546)(gcy-5::gfp)(rol-6).*

P_{flp-6}::wild-type-KVS-1 and P_{flp-6}::C113S-KVS-1 transgenic worms. The constructs were linearized and injected (3 ng/µl) into the syncitial gonads of adult *tm2034* hermaphrodites together with the two linearized transformation markers *myo-2::gfp* and *gcy-5::gfp* (3 ng/µl each) and 50 ng/µl of genomic DNA digested with Sca I [3].

Behavioral assays

Age-synchronization. Nematodes were grown in standard 10 cm NGM plates + OP50 *E. coli* until a large population of gravid adults was reached (3-5 days). The animals were collected in 50 ml Falcon tubes, washed in M9 buffer (22 mM KH_2PO_4, 22 mM NaH_2PO_4, 85 mM NaCl, 1 mM $MgSO_4$), and treated with 10 volumes of basic hypochlorite solution (0.25 M NaOH, 1% hypochlorite freshly mixed; no significant differences were observed in bleach-free preparations, obtained by isolating laid eggs with SDS/NaOH). Worms were incubated at room temperature for 10 minutes, then the eggs (and carcasses) collected by

centrifugation at 400g for 5 minutes at 4 °C, incubated overnight in M9 buffer and seeded on standard NMG plates.

Behavioral tests were performed without knowledge of the worms' genotype.

A) Chemotaxis assays. Experiments were performed as described previously [2]. Briefly, a chunk of agar 0.5-cm in diameter was removed from 10-cm plates and soaked in the attractant for 2 hours. Lysine and biotin were used at concentrations of 0.5 M and 0.2 M, respectively. Chunks were put back in the plate overnight to allow equilibration and formation of a gradient. Roughly 20 age-synchronized worms were placed between the test spot and a control spot on the opposite side of the plate. 10 µl of 20 mM NaN3 was placed on both spots. After one hour, animals on the test/control spot were counted, and a chemotaxis index, C.I., calculated as the number of animals at the test spot (N_{test}) minus the number of animals at the control spot ($N_{Cnt.}$), divided by the total number of animals (N). A positive C.I. indicates attraction:

$$C.I. = \frac{N_{Test} - N_{Cnt.}}{N} \qquad \text{(S-3)}$$

An experiment was carried out with roughly 100 worms/genotype distributed in 5 test plates.

To study chemotaxis during ageing, experiments were started with ~600-1000 age-synchronized worms per genotype (mean life span ~ 20 days). Worms were examined every day until death and were scored as dead when they were no

longer able to move even in response to prodding with a platinum pick. Each day, worms were transferred to a fresh plate containing bacteria. The experiments with Pflp-6::wild-type-KVS-1 and Pflp-6::C113S-KVS-1, were started with ~200-300 age-synchronized worms.

B) Thrashing assay. Experiments were performed as described previously [2]. Briefly, age-synchronized worms were picked in a drop of M9 buffer on an agar plate. After 2 min of recovery, thrashes were counted for 2 min. A thrash was defined as a change in the body bend at the mid-body point.

C) Solid substrate assay. Worms were filmed using a digital Photometrics Cascade 512B camera connected to a Leica MZ16 microscope at a rate of 3 frames per second. Speed was calculated as the distance covered by a point located in the mid-body of the animal in one second. The average speed of a worm was calculated by averaging 10 or more individual measurements.

SOD assay

Worms were grown as described above, lysed in 50 mM TRIS-HCL (pH =8.0) and SOD activity was assessed using the Superoxide Dismutase Assay II kit (Calbiochem).

Electrophysiology

a. Heterologous expression systems

Data were recorded with an Axopatch 200B amplifier (Axon) a PC (Dell) and Clampex software (Axon). Data were filtered at f_c=1 kHz and sampled at 2.5 kHz. *Heterologus expression system*. Chinese Hamster ovary (CHO) and Human Embryonic Kidney 293 (HEK 293) cells were plated/transfected as described before [2] and used 24-36 hours post-transfection. Bath solution was (in mM): 4 KCl, 100 NaCl, 10 Hepes (pH=7.5 with NaOH), 1.8 $CaCl_2$ and 1.0 $MgCl_2$. Pipette solution: 100 KCl, 10 Hepes (pH=7.5 with KOH), 1.0 $MgCl_2$, 1.0 $CaCl_2$, 10 EGTA (pH=7.5 with KOH). CHT and DTT were added fresh prior the experiment from 1 M stocks in H_2O. Offset potentials due to series resistances (≤ 5 mV) were not compensated for when generating current-voltage relationships.

b. Primary cultures

Cultured ASER cells were prepared as described before [4]. Briefly, gravid adult worms were lysed using 0.5 M NaOH and 1% NaOCl (no significant differences were observed in bleach-free preparations, obtained by isolating laid eggs with SDS/NaOH). Released eggs were washed three times with sterile egg buffer containing 118 mM NaCl, 48 mM KCl, 2 mM CaCl2, 2 mM MgCl2, and 25 mM Hepes (pH 7.3, 340 mosM), and adult carcasses were separated from washed eggs by centrifugation in sterile 30% sucrose. Eggshells were removed by resuspending pelleted eggs in a sterile egg buffer containing 1 unit/ml chitinase at room temperature for 1.5 hours. Embryos were resuspended in L-15 cell culture medium containing 10% fetal bovine serum, 50 units/ml penicillin, and 50 µg/ml streptomycin (Sigma) and dissociated by gentle pipetting. Intact embryos,

clumps of cells, and larvae were removed from the cell suspension by filtration. Dissociated cells were plated on glass cover slips previously coated with peanut lectin (0.1 mg/ml) dissolved in water. For electrophysiological recordings bath solution was (in mM): 145 NaCl, 5 KCl, 1 $CaCl_2$, 5 $MgCl_2$, 10 Hepes/NaOH (pH =7.50, and 20 D-glucose. Pipette solution: 125 potassium gluconate, 18 KCl, 0.7 $CaCl_2$, 2 $MgCl_2$, 2 MgATP , 10 EGTA/KOH, and 10 Hepes/KOH (pH = 7.5). Currents were repeatedly elicited 3-5 times (with the same voltage-stimulus) and digitally averaged on line. Leak currents were recorded in the cell-attached configuration before establishing the whole-cell configuration and were digitally subtracted during analysis. Offset potentials due to series resistance (≤ 2 mV) were not compensated for when generating current-voltage relationships.

References

1. Cai, S.Q. and F. Sesti, *A new mode of regulation of N-type inactivation in a Caenorhabditis elegans voltage-gated potassium channel.* J Biol Chem, 2007. **282**(25): p. 18597-601.
2. Bianchi, L., S.M. Kwok, M. Driscoll, and F. Sesti, *A potassium channel-MiRP complex controls neurosensory function in Caenorhabditis elegans.* J Biol Chem, 2003. **278**(14): p. 12415-24.
3. Evans, C.T., ed. *Transformation and microinjection*. Wormbook, ed. T.C.e.R. Community. 2006.
4. Park, K.H., L. Hernandez, S.Q. Cai, Y. Wang, and F. Sesti, *A Family of K+ Channel Ancillary Subunits Regulate Taste Sensitivity in Caenorhabditis elegans.* J Biol Chem, 2005. **280**(23): p. 21893-9.